Available online at www.sciencedirect.com
SCIENCE DIRECT®
Journal of Nuclear Materials 319 (2003) 102–107
journal of nuclear materials
www.elsevier.com/locate/jnucmat

In-pile irradiation of rock-like oxide fuels

N. Nitani *, K. Kuramoto, T. Yamashita, Y. Nihei, Y. Kimura

Japan Atomic Energy Research Institute, Tokai, Ibaraki 319-1195, Japan

Abstract

Five kinds of rock-like oxide fuels were prepared and irradiated using 20% enriched U instead of Pu. The microstructure analyses for irradiated fuel pellets were carried out by ceramography and electron probe microanalysis (EPMA). For $MgAl_2O_4$ (spinel)-based fuel, decomposition of the spinel and vaporization of MgO (magnesia) was observed. For Al_2O_3 (corundum)-based fuels, significant appearance changes were not observed under the irradiation condition of sufficiently high fuel temperature. Fission product (FP) distributions were also analyzed by EPMA. The distributions of Nd and Ba were similar with those of U and Zr. Mo and Pd were found as fine inclusions in the yttria-stabilized zirconia (YSZ) phase. A part of Cs and Xe migrated to the periphery of YSZ particles and to pores in YSZ. The FP distributions of spinel-based fuel were almost similar to corundum-based fuel.
© 2003 Elsevier Science B.V. All rights reserved.

1. Introduction

The concept of the rock-like oxide (ROX) fuel has been developed for the annihilation of excess plutonium in light water reactors (LWRs). Features of the ROX-LWR system are almost complete burning of plutonium and the direct disposal of spent ROX fuels without reprocessing [1]. The ROX fuel consists of such phases as yttria-stabilized zirconia (YSZ, $(Y, Zr)O_{2-x}$), spinel ($MgAl_2O_4$) and corundum (Al_2O_3). Plutonium, other actinides and lanthanide fission products (FPs) are dissolved into the YSZ. The roles of spinel or corundum are to immobilize alkali and alkaline earth nuclides and to improve thermal conductivity. In a previous study, in-pile irradiation examination for plutonium ROX fuel disks with a ternary system of YSZ, corundum and spinel was carried out. The existence of excess corundum caused unfavorable behaviors, such as large swelling and high FP gas release [2].

For the improvement of swelling behavior, a particle-dispersed type fuel was proposed [3]. When YSZ particles of appropriate size are dispersed homogeneously in the spinel or corundum matrix, the damaged area of the matrix is limited to thin layers surrounding the particles. Fuel pellets with <10% porosity including UO_2 containing YSZ (U-YSZ) particles were fabricated using a conventional process [3].

The irradiation test was performed in order to confirm the effect of the particle-dispersed type fuels on irradiation resistance. The ROX fuel of YSZ and spinel system, which was the most promising composition was used to the experiment. The fuel of YSZ and corundum system was also irradiated, because it was expected that the swelling of corundum is reduced on particle dispersed type fuel. Moreover, the homogeneously blended type fuels were irradiated to compare the irradiation behavior.

In this study, the microstructure analyses for irradiated fuel pellets were carried out by ceramography and electron probe microanalysis (EPMA), and FP distributions in fuel pellets were obtained. The results of the examination will be described and discussed.

2. Experimental

2.1. Preparation of fuels

Five kinds of fuels were prepared using 20% enriched U instead of Pu; a single phase fuel of U-YSZ (Z), two particle-dispersed type fuels of U-YSZ particles in spinel

* Corresponding author. Tel.: +81-29 282 6939; fax: +81-29 282 6805.
E-mail address: noriko@popsvr.tokai.jaeri.go.jp (N. Nitani).

0022-3115/03/$ - see front matter © 2003 Elsevier Science B.V. All rights reserved.
doi:10.1016/S0022-3115(03)00140-5

Table 1
Fuel compositions (mol%)

Fuel type	Solid solution	Particle-dispersed[a]		Homogeneously blended[b]	
Compound I	$(Y, U, Zr)O_{2-x}$	$(Y, U, Zr)O_{2-x}$	$(Y, U, Zr)O_{2-x}$	$(Y, U, Zr)O_{2-x}$	$(Y, U, Zr)O_{2-x}$
Compound II		$MgAl_2O_4$	Al_2O_3	$MgAl_2O_4$	Al_2O_3
Fuel	Z	SD	CD	SH	CH
ZrO_2	64.23	9.35	9.38	9.35	9.38
$YO_{1.5}$	17.52	2.55	2.56	2.55	2.56
UO_2	18.25	19.71	19.76	19.71	19.76
$AlO_{1.5}$	—	45.60	68.31	45.60	68.31
MgO	—	22.79	—	22.79	—

[a] Particle size: 250 μm.
[b] Grain size: 10–50 μm.

or corundum matrix (SD or CD), two homogeneously blended type fuels of U-YSZ and spinel or corundum (SH or CH). The compositions of these fuels are shown in Table 1. The atom density of ^{235}U is designed as 10^{27} m^{-3} in all fuels. The U-YSZ particles in particle-dispersed fuel pellets were fabricated by an external sol–gel process [3]. The size of U-YSZ particles was about 250 μm in diameter. The homogeneously blended type fuels and the U-YSZ single phase fuel were fabricated by mixing oxide powder of each component. All fuel pellets were sintered at 2020 K for 4 h in a stream of $75\%H_2/25\%N_2$ mixed gas. The size of each pellet was about 5.3 mm in diameter and 5.5 mm in height.

2.2. Irradiation

These fuels were irradiated in the Japan Research Reactor No. 3 (JRR-3) for about 100 d. Nominal reactor power was 20 MW and maximum neutron fluence was estimated to be about 7×10^{24} m^{-2}. The linear power was estimated from the activity measurement of fluence monitors placed close to each fuel pin. The surface and center temperatures of fuel pellets were estimated from obtained linear power. Estimated linear power and temperature of each fuel are listed in Table 2. It must be mentioned that the temperature of each fuel is remarkably higher than that of irradiation condition in LWRs, Except for Z fuel that irradiated at the bottom of the capsule.

The results of burnup calculation by SRAC95 code system are also shown in Table 2. The estimated burnups are about 100 GW d m^{-3}, which is corresponding to about 10 GW d t^{-1} of LWR UO_2 fuel.

3. Results and discussion

3.1. Microstructures of fuel pellets

The non-destructive post-irradiation examinations (profilometry, X-ray radiography and γ scanning) and some destructive examinations (puncture test, fission gas analysis) were carried out earlier. The results were described and discussed elsewhere [4,5].

The microstructure analyses of irradiated fuel pellets were carried out by ceramography and EPMA. The SEM images of Z, SD, SH, CD and CH fuels are shown in Fig. 1. In the Z and CH fuel pellets, several radial cracks existed, as similarly observed in the LWR UO_2 fuel. The pellets showed uniform structure throughout the fuel surface. No apparent microstructure changes were found in these fuels, although the central region of the pellets revealed a slightly porous microstructure. From X-ray diffraction analysis, deformation of the diffraction peak or phase separation of the fluorite phase was not observed. The dark regions seen in CH fuel are not pores, but large grains of corundum. The aspects of outer region of SD and SH resemble those of CD and CH, respectively. In the SD and SH fuel pellets, about 0.5 mm diameter central holes were formed during irradiation (see Fig. 1(b) and (c)). The U-YSZ particles of the SD fuel were concentrated to the center of the pellet,

Table 2
Estimated irradiation condition and burnup of the fuels

Fuel	Z	SD	CD	SH	CH
Linear power (kW m^{-1})	13.9	23.0	24.9	23.4	20.7
T surface of pellet (K)	990	1250	1300	1440	1290
T center of pellet (K)	1490	1740	1820	1940	1730
Burnup (^{235}U%)	21.01	23.28	23.89	24.15	20.87
Burnup (GW d m^{-3})	59	100	105	103	88

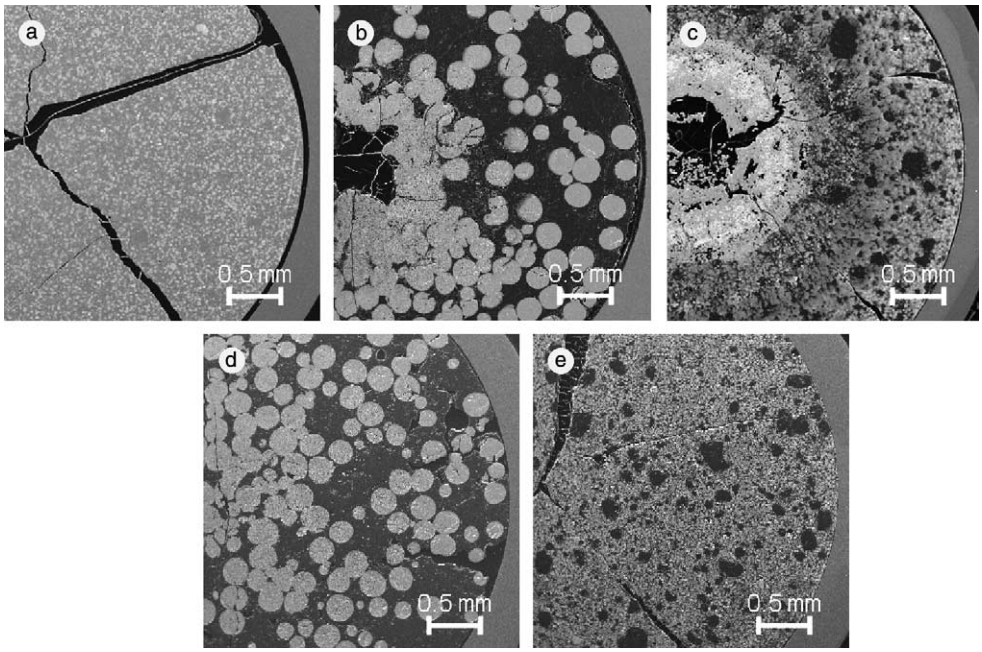

Fig. 1. The SEM images of (a) Z ((Y, U, Zr)O_{2-x}), (b) SD ((Y, U, Zr)O_{2-x} + $MgAl_2O_4$, particle-dispersed), (c) SH ((Y, U, Zr)O_{2-x} + $MgAl_2O_4$, homogeneously blended), (d) CD ((Y, U, Zr)O_{2-x} + Al_2O_3, particle-dispersed) and (e) CH ((Y, U, Zr)O_{2-x} + Al_2O_3, homogeneously blended) fuels.

and the particles were deformed possibly due to sintering. This behavior, the aggregation of U-YSZ grains, was also observed for the SH fuel. The fuel structures and components varied concentrically, and many pores were generated in central and intermediate regions. On the other hand, the deformation and the aggregation of the U-YSZ particles was rarely observed for CD fuel. The CD fuel pellet showed uniform structure throughout the pellet surface, similar to Z and CH fuel pellets.

The line profiles of U, Zr, Al and Mg for SD fuel and those of U, Zr and Al on CD fuel are shown in Fig. 2 with a SEM image. By comparing the distributions of Al and Mg on SD fuel, it was confirmed that Al existed not as spinel but as corundum in the region towards the center of the pellet. The irradiated SD fuel pellet comprised roughly three regions; the center region consisted only of U-YSZ (about 0.5–1.2 mm from the center of the pellet); the middle region consisted of U-YSZ and corundum (about 1.2–1.7 mm); the outer region consisted of the original U-YSZ and spinel (about 1.7 mm-surface). The observed appearance changes by irradiation were smaller in the outer region. A similar feature was observed in the SH fuel. Magnesia was detected on the pellet surface and the cladding tube.

It is considered that the occurrence of corundum phase in the SD and SH fuel was caused by the decomposition of spinel by fission damage and vaporization of magnesia. The resistance of spinel to neutron irradiation is high [6], but that to fission fragment might be not sufficient. High irradiation temperature and large temperature gradient ($\sim$200 K mm^{-1}) caused the magnesia vaporization, because the vapor pressure of magnesia was higher by about 5 orders of magnitude than that of corundum. In high temperature and irradiation field, magnesia produced by decomposition of the spinel was vaporized, and moved to the gap and deposited there at lower temperature. By the vaporization of the magnesia, the spinel was transformed into corundum. The volume of matrix decreased by the transformation. The central hole of the pellet was caused by migration of voids, which were generated by the volume reduction of the matrix. The U-YSZ grains, which are present in the central area of the pellet, were displaced and were aggregated by central hole generation.

We estimated the temperature distributions in the fuel pellets during irradiation assuming the initial thermal conductivities of the respective matrices. By comparing the aspect of pellet surface and the temperature distribution, it is expected that the vaporization of magnesia occurred in the area where the fuel temperature was over about 1700 K. In the region below 1700 K, neither spinel decomposition nor restructuring was observed. It is expected that the vaporization of magnesia could be avoided by lowering the fuel temperature.

The distributions of the matrix elements for CD fuel were homogeneous from the center to the outer region.

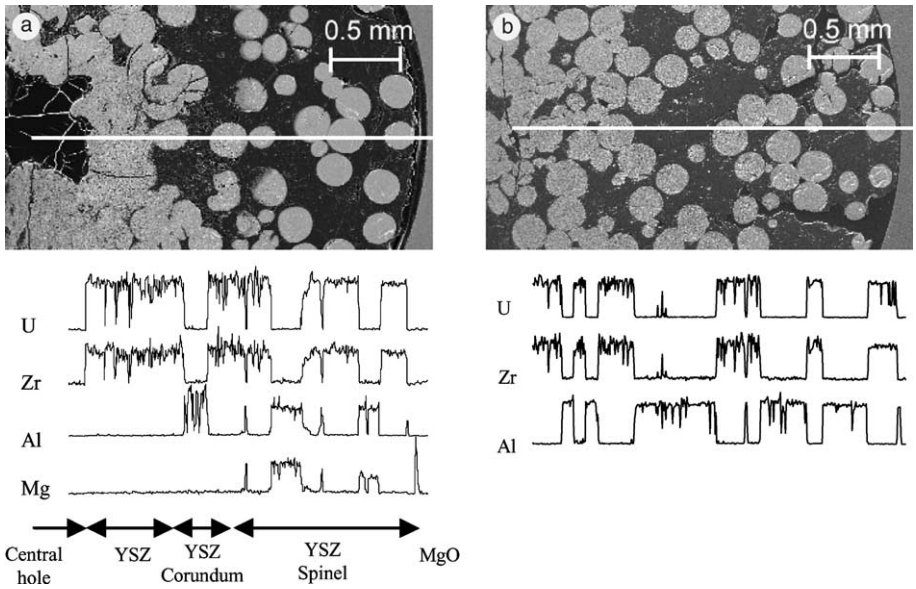

Fig. 2. The line profiles of U, Zr, Al and Mg and SEM image corresponds to the position measurement was carried out. White line shows the analyzed position. (a) SD fuel and (b) CD fuel.

It is known that the neutron resistance of corundum is inferior to that of spinel, and corundum becomes amorphous by fission damage. The amorphization causes a large volume swelling in low temperature region of the fuel [7]. In this work, the swelling of the fuel was small [5], and no amorphization was observed by X-ray diffraction. It is considered that the damaged crystal structure recrystallized, because the irradiation temperature was high enough to anneal the amorphous corundum. No central holes were observed in corundum-based fuel pellets. Because the volume change by the irradiation of the corundum was smaller than that of the spinel in which magnesia vaporization occurred, the amount of generated void in the corundum-based fuel was less than that in the spinel-based fuel.

3.2. FP distribution

The microstructures around the boundary between U-YSZ particles and matrix were examined in further detail. The elemental mapping was carried out using EPMA for matrix and FP elements. For spinel-based fuel, we intended to confirm the influence of the spinel restructuring on FP distributions. The FP elements which have different chemical properties were selected for the analysis; Nd, Ba, Mo, Ru, Cs and Xe.

The SEM image of the outer region of SD fuel pellet is shown in Fig. 3(a). That is the region where no vaporization of magnesia occured. A gray layer of about 10 μm thickness can be observed at the surface of the particle. The layer consists of fine grains of spinel and U-YSZ. The thickness of the layer is comparable to the mean range of fission fragments. In the irradiation field, the spinel and the YSZ grains segmented to fine grains. The layer probably indicates the radiation damaged region. Fig. 3(b)–(j) are element distributions mapped by EPMA at the same region as shown in Fig. 3(a). White points show the points where the element exists. All matrices elements, Fig. 3(b)–(e), are present in the reaction layer.

FP distributions of SD fuel are shown in Fig. 3(f)–(j). The distribution of Nd and Ba is similar with those of U and Zr, and it is confirmed that Nd and Ba were immobilized by the U-YSZ phase. A part of Cs and Xe concentrated in pores in the YSZ. The aggregation to the boundary region between U-YSZ particle and matrix is also observed for Cs and Xe. It is supposed that these elements could migrate more easily due to generation of the reaction layer. Although the migration to the periphery of YSZ particles occurs, its influence is negligible if crack formation is prevented.

Fig. 4(a) is an SEM-image of the outer region of the CD fuel. Different from SD fuel, no layer was observed for the CD fuel, neither in the SEM-image nor in the EPMA-distributions of matrices and U, as shown in Fig. 4(b)–(d). FP distributions of CD fuel are shown in Fig. 4(e)–(h). The distribution of Nd was similar with those of U and Zr. Ru and Mo were found as fine inclusions in the U-YSZ phase. The FP distributions in CD fuel were analogous to those in SD fuel. However, no Cs and Xe migration to the periphery of YSZ particles was observed. Some Cs migrated to pores in YSZ and escaped

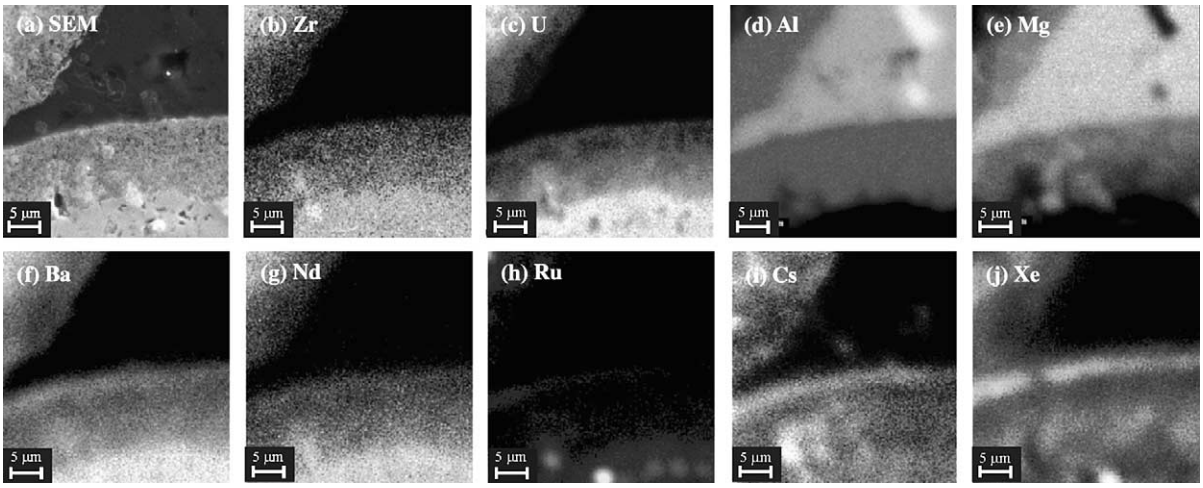

Fig. 3. Typical SEM image and characteristic X-ray pictures on the outer region of SD fuel (a) SEM, (b) Zr, (c) U, (d) Al, (e) Mg, (f) Ba, (g) Nd, (h) Ru, (i) Cs and (j) Xe.

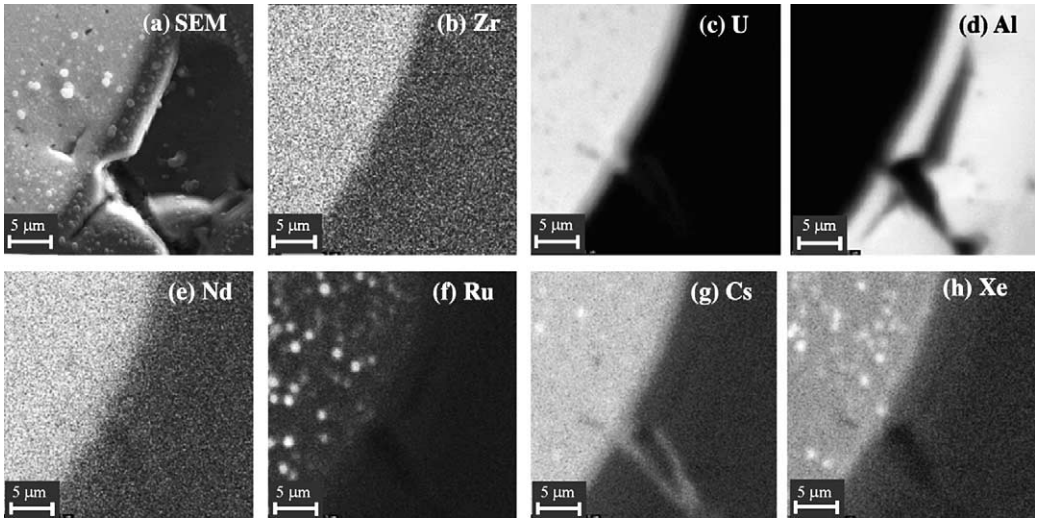

Fig. 4. Typical SEM image and characteristic X-ray pictures on the outer region of CD fuel (a) SEM, (b) Zr, (c) U, (d) Al, (e) Nd, (f) Ru, (g) Cs and (h) Xe.

through cracks in the matrix. Although some Xe migrated to pores and formed gas bubbles, most Xe remained in the YSZ phase. For CD fuel, the FP distributions at the center region were almost similar to that at the outer region, only the size of fine inclusions of Ru and Mo became larger, because of the higher fuel temperature.

SEM image and element distributions in the middle region of SD fuel are shown in Fig. 5. In this region, vaporization of magnesia and subsequent restructuring occurred, and fuel particle deformation took place. The boundary between matrix and the fuel particle is extremely unsmooth, the pores in the fuel particles grew to a few micrometers in diameter. Magnesium was detected only in traces (Fig. 5(e)). Because of the large pore size, the Xe and Cs that gathered in pores might have escaped, either through cracks during irradiation or during sample preparation. However, in either case, it is confirmed by the EPMA mapping of Xe and Cs that much Xe and Cs remained in the YSZ. Although the appearance of the fuel particles was changed extremely, the changes of FP distribution were little and much FP remained in the YSZ phase.

In the SD fuel where magnesia vaporization occurred and in the whole CD fuel, a new hibonite structure was observed. The plate-like grains seen in Fig. 5(a), identified

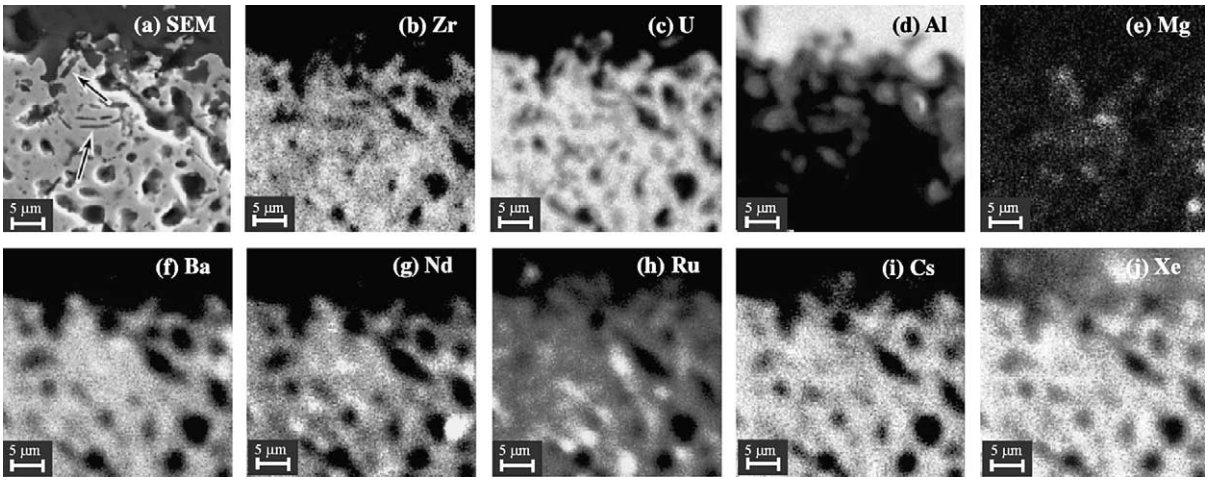

Fig. 5. Typical SEM image and characteristic X-ray pictures on the middle region of SD fuel (a) SEM, (b) Zr, (c) U, (d) Al, (e) Mg, (f) Ba, (g) Nd, (h) Ru, (i) Cs and (j) Xe.

by arrows, are the hibonite phases. The components of the hibonite are obscure on the EPMA mapping shown in Fig. 5, but they were analyzed qualitatively by using energy dispersive spectroscopy at the center point of the phase. It was confirmed that the hibonite consists of Ba ($BaAl_{12}O_{19}$) or Nd ($NdAl_{11}O_{18}$, $NdMgAl_{11}O_{19}$). Therefore almost all magnesium present in the depicted region formed hibonite, not spinel. The hibonite might be the host phase of trivalent actinide elements such as Pu and Am. In practice, the hibonite formation with Pu ($PuMgAl_{11}O_{19}$) has been observed in a previous study. Although many properties of hibonite are unknown, it is reported that hibonite has sufficient chemical durability from the geological safety point of view [8]. Hence the formation of hibonite is not necessarily disadvantage.

4. Conclusion

Five kinds of ROX fuels were irradiated and post-irradiation examinations were carried out.

The microstructures of fuels were analyzed by ceramography and EPMA. The aspect of the Z fuel pellet was analogous to LWR UO_2 fuels, and showed uniform structure throughout the pellet surface.

It was confirmed that the decomposition of spinel and vaporization of magnesia occurred due to the high temperature irradiation, for the spinel-based fuels. It is expected that the vaporization of magnesia can be avoided by lowering the fuel temperatures to less than 1700 K.

For corundum-based fuels, under this irradiation condition of sufficiently high irradiation temperature to anneal the amorphous corundum, no significant appearance changes such as swelling and heterogeneity of fuel structures were observed.

FP distributions were also examined by EPMA. The distributions of Nd and Ba were similar with those of U and Zr. Ru and Mo were found as fine inclusions in the YSZ phase. A fraction of Cs and Xe migrated to the periphery of YSZ particles and to pores in YSZ.

The FP distributions of spinel-based fuel were mostly similar to corundum-based fuel. Although the fuel microstructure was altered considerably, the changes of FP distribution were small and much remained in the YSZ phase for the region where vaporization of magnesia and subsequent restructuring occurred.

References

[1] H. Akie, T. Muromura, H. Takano, S. Matsuura, Nucl. Technol. 107 (1994) 182.
[2] T. Yamashita, N. Nitani, H. Kanazawa, M. Magara, T. Ohmichi, H. Takano, T. Muromura, J. Nucl. Mater. 274 (1999) 98.
[3] T. Shiratori, T. Yamashita, T. Ohmichi, A. Yasuda, K. Watarumi, J. Nucl. Mater. 274 (1999) 40.
[4] N. Nitani, K. Kuramoto, T. Yamashita, Y. Nakano, H. Akie, Proceedings of International Conference on Back-end of the Fuel Cycle: from Research to Solutions (Global-2001), Paris, France, 11–14 September 2001, p. 018.
[5] T. Yamashita, K. Kuramoto, H. Akie, Y. Nakano, N. Nitani, T. Nakamura, K. Kusagaya, T. Ohmichi, J. Nucl. Sci. Technol. 39 (2002) 865.
[6] R.J.M. Konings, K. Bakker, J.G. Boshoven, R. Conrad, H. Hein, J. Nucl. Mater. 254 (1998) 135.
[7] R.M. Berman, M.L. Bleiberg, W. Yeniscavich, J. Nucl. Mater. 2 (1960) 129.
[8] T. Yanagi, Y. Makino, K. Kuramoto, S. Muraoka, J. Nucl. Sci. Technol. 31 (1994) 1092.